



Millington, O. R., Brewer, J. M., Garside, P., and Maffia, P. (2010) *Imaging interactions between the immune and cardiovascular systems in vivo by multiphoton microscopy*. In: Marelli-Berg, F. M. and Nourshargh, S. (eds.) *T-Cell Trafficking: Methods and Protocols*. Series: *Methods in Molecular Biology*, 616 (616). Humana Press Inc, pp. 193-206. ISBN 9781607614609

Copyright © 2010 Humana Press Inc.

A copy can be downloaded for personal non-commercial research or study, without prior permission or charge

Content must not be changed in any way or reproduced in any format or medium without the formal permission of the copyright holder(s)

<http://eprints.gla.ac.uk/46003/>

Deposited on: 15 December 2014

Enlighten – Research publications by members of the University of Glasgow
<http://eprints.gla.ac.uk>

Imaging interactions between the immune and cardiovascular systems *in vivo* by multiphoton microscopy

Running head: *In vivo* imaging of immunity in atherosclerosis

Owain R. Millington PhD^{1,2}, James M. Brewer PhD^{1,2}, Paul Garside PhD^{1,2}, Pasquale Maffia PhD^{2,3,4}

¹ Centre for Biophotonics, ² Strathclyde Institute of Pharmacy & Biomedical Sciences, University of Strathclyde, Glasgow G4 0NR, U.K.; ³ Department of Experimental Pharmacology and ⁴ School of Biotechnological Sciences, University of Naples Federico II, 80131 Naples, Italy.

Correspondence to: Owain Millington, Centre for Biophotonics, Strathclyde Institute of Pharmacy & Biomedical Sciences, University of Strathclyde, 27 Taylor Street, Glasgow G4 0NR, UK, Tel: +44 (0)141 548 3895, Fax: +44 (0)141 552 2562, E-mail: owain.millington@strath.ac.uk

i. Summary/Abstract

Several recent studies in immunology have used multiphoton laser-scanning microscopy to visualise the induction of an immune response in real time *in vivo*. These experiments are illuminating the cellular and molecular interactions involved in the induction, maintenance and regulation of immune responses. Similar approaches are being applied in cardiovascular research where there is an increasing body of evidence to support a significant role for the adaptive immune system in vascular disease. As such, we have begun to dissect the role of T lymphocytes in atherosclerosis in real time *in vivo*. Here, we provide step-by-step guides to the various stages involved in visualising the migration of T cells within a lymph node and their infiltration into inflamed tissues such as atherosclerotic arteries. These methods provide an insight into the mechanisms involved in the activation and function of immune cells *in vivo*.

ii. Key Words

Brachiocephalic artery, Imaging, Lymph node, Multiphoton Microscopy, T cells.

1. Introduction

Atherosclerosis has been recognised as an inflammatory disease and much of the current research is focused on investigating how this inflammation is regulated. Adaptive immunity is highly involved in atherogenesis (*1, 2*), but we still have much to learn about its effective role in the pathology. The adaptive immune system is a complex collection of cells, that interact in distinct locations in a tightly regulated manner in order to allow the rapid induction of immunity and prevent the induction of inappropriate responses. Failure of this regulation is associated with development of many inflammatory and autoimmune diseases such as atherosclerosis and rheumatoid arthritis. Importantly, the stochastic generation of antigen receptor diversity produces a low frequency of antigen-specific cells. In order to provide effective immune surveillance, these cells must therefore migrate throughout the body in search of cognate antigen presented upon dendritic cells (DCs). The contact between an antigen-presenting cell and a naïve T cell can have important consequences for the induction of immunity since failure to establish stable cell-cell interactions prevents the optimal activation of T cell responses (*3-6*), which may be of benefit in therapeutic applications. Analysing the cellular interactions during the induction, maintenance and effector stages of an immune response therefore provides insight into how antigen-specific immunity may be manipulated for therapeutic benefit. Indeed, molecules involved in these interactions (such as CTLA-4, CD28 and CD3) have recently been targeted for therapeutic use.

Whilst a range of imaging techniques have been applied to immunology over recent years, few have provided such an insight into the cellular interactions involved in the induction of immune responses as multiphoton laser-scanning microscopy (MPLSM) (*3-16*). Studies using MPLSM have demonstrated that naïve T cells show

rapid motility within the lymph node (LN), contacting multiple DCs per hour, allowing them to effectively scan for antigen (7-9). Following antigen recognition, T cells reduce their velocity and remain associated with the antigen-presenting DC (8-10). The dynamics and kinetics of this interaction have important implications in the induction of immunity, with a stable interaction being required for effective T cell priming, whereas shorter/less contact results in the failure of immunity and/or tolerance (3-6). More recently, the role of specific molecules involved in the activation and regulation of these DC:T cell interactions have been investigated, providing a mechanistic insight into immune activation (11, 17). However, in the majority of inflammatory-based pathogenesises, it is the somatic tissues which are the target of disease. Whilst many important studies have investigated the role of cells within the LNs or in the tissues of these diseases, few have examined the interaction between these sites. Thus, it is often assumed that observations made in the LN apply to cells in the tissue and vice-versa (e.g. *in vivo* observations of CTL activity, which may not carry out killing in the LN under normal conditions). Clearly, this may not actually be the case, and therefore it is important to examine the cellular behaviour of cells in the tissue AND in the LN and eventually to image the migration between them. As such, we have begun to investigate the relationships between the immune and cardiovascular systems by imaging the LN and artery (16) in real time *in vivo*. Lymphocytes infiltrate the arterial wall before and during development of atherosclerosis (16, 18), but we still need to investigate their potential antigens, their contact-dependent activities and cross-talk with other cells within or outside the atherosclerotic vessels. A major hurdle is the limited knowledge regarding secondary lymphoid tissue where priming of atherogenic T cells should take place, such as the draining LNs. Thus, imaging immune cell behaviour directly in intact atherosclerotic

vessels, as well as the associated lymphoid tissues (if any) could provide important information for the development and use of immune specific therapies in vascular pathology, as well as an improved understanding of the migration and interactions of cells involved in immune pathology.

Here we provide a description of how samples are prepared for imaging in order to analyse the behaviour of T cells *in vivo* not only within the lymph node but also a potential target tissue, the atherosclerotic blood vessel. Whilst most studies to date have used adoptively transferred populations of antigen-specific T cells, there is an increasing use of mice in which fluorescent reporters are expressed by specific subsets of cells or induced under certain conditions and these could be used in the following protocols. Unfortunately, there are currently few MPLSM systems that provide the tuneable excitation laser, accurate scan head and sensitive detection system essential for *in vivo* imaging. Hence, most groups use customised microscope systems along with environmental control systems to maintain tissue viability. The methods and notes described here should help in establishing imaging systems for the visualisation of T cell migration within the lymph node and the target tissue it drains.

2. Materials

2.1. Mice

A selection of mice have been used in MPLSM imaging experiments, depending on the exact experimental question. Commonly, T cell receptor (TCR) transgenic animals are used as donors for adoptive transfer, allowing the visualization of a population of antigen-specific T cells in the recipient animal. Typically, we have used the ovalbumin (OVA)-specific DO11.10 mice on a *scid* background. Since these mice are unable to generate T or B cells of any other specificity, we can be sure that all the

cells analyzed are the antigen-specific cells of interest. Alternatively, CD4/CD8 T cell isolation must be performed (19). For vascular imaging, C57BL6 or OVA-specific OT-II mice (on a C57BL6 background) are used as lymphocyte donors for adoptive transfer and Apolipoprotein E deficient mice (ApoE^{-/-}, B6.129P2-ApoE^{tm1Unc}), showing a marked increase in total plasma cholesterol levels, as recipient animals. In these animals, monocyte attachment to endothelial cells is observed at 6 weeks, foam cell lesions develop as early as 8 weeks and fatty streaks in the proximal aorta and carotid are found at 3 months of age. The lesions increase with age and progress to lesions with less lipid but more elongated cells, typical of a more advanced stage of pre-atherosclerotic lesion.

2.2. CFSE and CMTPX stock

5- (and-6-) carboxyfluorescein diacetate, succinimidyl ester (5(6)-CFDA, SE; Invitrogen, Paisley, U.K.) is prepared as a 10 mM stock solution in DMSO and kept frozen at -20°C in aliquots.

Cell TrackerTM Red CMTPX (Invitrogen) is prepared as a 20 mM stock solution in DMSO and kept frozen at -20°C in aliquots.

2.3. Media

RPMI 1640 (Sigma-Aldrich, Poole, U.K.).

HBSS (Sigma-Aldrich).

Complete medium [RPMI 1640, 10% Foetal calf serum (FCS), 2 mM L-glutamine, 100 U/mL penicillin, 100 mg/mL streptomycin, 1.25 mg/mL fungizone; all obtained from Invitrogen].

CO₂-independent medium (Invitrogen).

2.4. Other items

Nitex membranes (Cadisch & Sons, London, U.K.) or 40 µm cell strainers (BD Bioscience, Oxford, U.K.).

Plastic coverslips.

3M™ Vetbond™ Tissue Adhesive 1469SB.

3. Methods

3.1. Removal of Lymph Nodes

1. Cull the mouse with an increasing concentration of CO₂.
2. Spray the mouse with 70% ethanol to prevent fur from contaminating the region to be dissected.
3. Lie the cadaver ventral side up, pin the mouse's paws to the dissection board and place under a light source.
4. Make an incision in the skin of the mouse from the abdomen to mandible.
5. Make further incisions from the central one towards each paw.
6. Separate skin from the abdominal muscles and pin out.
7. Dissect lymph nodes (e.g. inguinal, brachial, axillary, cervical and mesenteric) and spleen if required (see **Note 1**).

3.2. Preparation for adoptive transfer

1. Harvest peripheral and mesenteric LNs from donor mice into RPMI 1640.
2. Mash the LNs through Nitex mesh or BD cell strainers into 50 mL tube, using a syringe plunger.
3. Wash fresh media through the Nitex to fill the tube.

4. Spin the cells at 400g for 5 minutes and resuspend the pellet in an appropriate volume of HBSS for counting cells (see **Note 2**).
5. Count the cells using Trypan blue and a haemocytometer.
6. Spin the cells again and resuspend at a concentration of 10^7 lymphocytes per mL in appropriate pre-warmed buffer containing dyes.
 - a. If labelling cells with CFSE, resuspend in HBSS
 - b. If labelling with CMTPX, resuspend in CO₂-independent media
 - c. Add 0.5 μ L of stock CFSE/CMTPX per mL of buffer (see **Note 3**)
7. Immediately transfer cells to 37°C water bath and incubate with occasional agitation to prevent cell aggregation.
 - a. For CFSE (0.5 μ L stock solution/ 1×10^7 cells/mL) labelling, incubate for 10--15 minutes at 37°C (loose lid)
 - b. For CMTPX (0.5 μ L stock solution/ 1×10^7 cells/mL) labelling, incubate for 45 minutes at 37°C (loose lid)
8. Wash cells by topping up tube with FCS-containing buffer and centrifuging at 400g for 5 minutes (see **Note 4**).
9. Resuspend pellet in RPMI 1640 and count cells using Trypan blue.
10. Spin cells and resuspend at appropriate cell concentration for adoptive transfer (see **Note 5**).
11. Transfer into congenic recipient mice by intravenous injection.

3.3. Preparation of LN for imaging

A step by step visual guide to LN imaging is shown in Figure 1 (**15**).

1. Collect the appropriate LN for imaging and place in CO₂-independent medium warmed to room temperature (see **Notes 6-8**).

2. When ready for imaging prepare the LN by rolling on paper towel (Fig. 1C). This dries the LN a little and also allows removal of any fat still attached to the LN.
3. Place a small drop of Vetbond glue onto the unbreakable plastic coverslip (Fig. 1D) and spread using the corner of tissue paper to give a very thin layer over the coverslip (Fig. 1E).
4. Add the LN onto the coverslip directly without rolling over the glue-covered surface. Press down gently on the LN with forceps to secure it onto the coverslip but avoid putting too much force on it and damaging the capsule (Fig. 1F) (see **Note 9**).
5. Cure the Vetbond by immersing in the CO₂-independent medium (Fig. 1G). The plastic coverslip can now be cut down to size in order to fit into the imaging chamber (Fig. 1H).
6. Apply a small amount of grease to the underside of the coverslip (Fig. 1I) to adhere it into the imaging chamber.

3.4. Preparation of Brachiocephalic Artery for Imaging

1. Cull and prepare the mouse as described above (section 3.1, point 1-3).
2. Make an incision in the skin of the mouse from the abdomen to the top of the thorax.
3. Open the abdominal wall below the ribcage.
4. Lift the sternum with tweezers and cut the diaphragm. Then cut away the lower part of the ribcage to partially expose the heart
5. Draw blood from the heart by sticking the needle of a 1 mL syringe into the apex of the left ventricle (see **Note 10**).

6. Make a small incision in the right atrium for drainage.
7. Stick a 10 mL syringe into the apex of the left ventricle and slowly flush the blood from the mouse with 10 mL of PBS.
8. Dry the mouse by turning it over and pressing it against paper towels; return to the ventral position and re-pin the appendages.
9. Place the mouse under a dissecting microscope.
10. Remove the remaining ventral part of the ribcage, carefully cut the right clavicle leaving the brachiocephalic artery and its branches intact (Fig. 2A). Using microdissection scissors, remove all of the fat from around the ascending aorta and brachiocephalic artery.
11. Remove the fat and tissue surrounding the heart.
12. Cut the brachiocephalic artery distal to where it branches into the right subclavian and right carotid and then cut it at its branching site from the aorta to disclose a Y--shaped specimen (Fig. 2B); place in PBS to clean (see **Note 11**).
13. Take the cleaned piece of the brachiocephalic artery and place in CO₂-independent media warmed to room temperature.
14. When ready for imaging place a small drop of Vetbond glue onto the unbreakable plastic coverslip and spread using the corner of tissue paper to give a very thin layer over the coverslip (Fig. 1D,E).
15. Glue down the tail of the Y--shaped specimen of brachiocephalic artery onto the coverslip first, and gently lower the artery down from the opposite limb to secure it to the slide. Proceed as described above (section 3.3, point 5-6).

3.5. Perfusion system

The tissue ready for imaging is placed in a custom-built perfusion system to bathe tissue in warmed, oxygenated medium. Unfortunately, no off-the-shelf product is currently suitable for this. However, individual components are relatively easy to combine into a system that allows control over the flow-rate, temperature and oxygenation of medium throughout the imaging period (**20**).

1. RPMI 1640 is pre-warmed in a microwave to around 60°C and added to the reservoir, where it is kept warm (see **Note 12**).
2. A mixture of 95% O₂, 5% CO₂ is bubbled through the warmed media at a slow, steady rate.
3. Medium is pumped into the imaging chamber (1.5 mL volume) at a flow rate of 1--2 mL per minute, ensuring adequate perfusion of medium/oxygen and removal of waste.
4. Set the inline heater to warm the media above 37°C and monitor the temperature in the imaging chamber. Adjust until the temperature is between 35°C and 36°C.

3.6. Microscopy

Again, few complete MPLSM systems are commercially available ready for use and many groups have customized existing systems for their own use. Of the reported setups used, several groups (**3, 4, 7, 9, 10, 20**) describe systems similar to ours, consisting of the following:

1. Solid-state, tunable titanium:sapphire laser system (Chameleon, Coherent Inc., Glasgow, U.K.).

2. The laser beam is routed into a multiphoton excitation laser scanning system (Radiance 2000MP, Bio-Rad Laboratories) through an upright microscope (E600-FN, Nikon).
3. The objective lens used for all imaging investigations is a CFi-60 Nikon Fluor 40X/0.8 NA water-dipping objective lens.
4. The sample is illuminated with 770-830 nm light, with ~210 fs pulse duration and 76 MHz repetition frequency (see **Note 13**).
5. Excited fluorescence passes through a laser blocking filter (E625SP, Chroma Technologies, Rockingham, VT) and detected with a multi-alkali cathode photo-multiplier tube (S20 PMT) in an external or nondescanned configuration as part of the Radiance 2000MP system.
6. A filter block can be used to separate fluorescence at 500-550nm (green dyes or autofluorescence) from higher emitted wavelengths (red labelled cells).
7. The scans are acquired with 500 lines per second and between 256 x 256 to 1024 x 1024 pixel boxes, for a frame rate of 1.95 fps (see **Notes 14-16**).

3.7. Analysis

Several image analysis software packages have been used in the analysis of MPLSM data including Imaris (Bitplane, Zurich, Switzerland), MetaMorph (Molecular Devices, Downingtown, PA), VideoSavant (IO Industries, Ontario, Canada), Picviewer (John Dempster, University of Strathclyde, Glasgow, U.K.), Adobe AfterEffects (San Jose, CA), ImageJ (NIH, Bethesda, MD) and Volocity (Improvision, Coventry, U.K.). Although many of these tools perform several similar analyses, Volocity software allows the visualization and rendering of images as well as the semi-automated quantitation of cell movement and behaviour within the 3D

images (Fig. 3). Whilst the exact measurements required depend on the data being analyzed, there are certain steps that are commonly used:

1. Objects (cells) are identified based on their fluorescence, identifying the centroid location of all the individual cells in the sample.
2. Objects are linked over time by tracking an object over at least 8 time points.
3. Many data sets can be generated simply by tracking--e.g. track velocity, displacement, meandering index, motility co-efficient.
4. It is also possible to measure the interaction between DC and T cell using the colocalization tool to identify green and red voxels. This represents the amount of interaction between cells in sample and varies in different conditions.
5. Results can be displayed in a variety of formats, including showing all tracks in an x, y, z plot, plotting the speed of individual cells or calculating the amount of interaction across the sample (Fig. 3).

4. Notes

1. The inguinal lymph node is typically found in the skin flap just above the leg and you can find it by looking at junction of blood vessels that run above it. Axillary lymph nodes are located right along a major blood vessel and sometimes dissection can be tricky because of bleeding. Superficial cervical LN along the side of the jaw muscles of the mouse should not be confused with salivary glands. Take care when isolating the mesenteric LN, since this is often associated with a lot of fatty tissue, which is not required.
2. If using large numbers of donors, it is often worth centrifuging the supernatant from the first wash as this can increase cell yield.

3. It is best to add the fluorescent dye to the appropriate buffer and vortex prior to using to resuspend the cells. There is occasionally precipitation of CMTPX in CO₂-independent medium and can require thorough vortexing to prevent clumping when added to cells.
4. The inclusion of FCS in the wash buffer is important to remove any remaining free fluorescent dye.
5. Typically transfer 2--5 x 10⁶ antigen-specific cells in a volume of 0.2 mL per recipient.
6. Care is required to avoid damaging the capsule of the LN to preserve structure. However, it is important to avoid collecting associated fat which can decrease the quality of images obtained. A good way to tell if fat is removed is to place the LN in medium; if there is any fat it will float.
7. Generally use the LN draining the site of antigen challenge (e.g. when immunizing subcutaneously in the footpad, image the popliteal LN).
8. Medium should be warmed to room temperature in advance. Lymph nodes can be harvested from several mice and maintained in CO₂-independent medium for several hours. Keep tissues at room temperature and avoid placing on ice.
9. Normally place the LN onto the slide in a transverse orientation (i.e. on its side, with an apparent 'kidney' shape)
10. Draw blood by slowly pulling the plunger, twisting the needle. Do not draw for longer than a minute as blood will start to clot.
11. When handling the brachiocephalic artery, it is important to touch only at its ends and not in the middle to avoid damaging the adventitial layer.

12. Heating the medium as gas is bubbled through it helps prevent the build up of bubbles in the imaging chamber after the inline heater. These bubbles can often form on the tissue or objective lens, obscuring the images.
13. Excitation wavelengths from the Ti:sapphire laser are in the range 770--830nm, depending on fluorochrome. For single colour (CFSE) and/or autofluorescence imaging, excitation around 770--780nm is used. For imaging both CFSE and CMTPX-labelled cells, excitation is at 830nm. Green autofluorescence of adventitial connective tissue and elastin fibers in the arterial media is always visible in the range 770--830nm. Depending on laser power, green autofluorescence of superficial tissue nuclei can be detected at an excitation of 770--780nm.
14. When setting up LN for imaging, focus to the top of the LN and then z-step down through the tissue to image at a known depth. Typically this is around 200--500 μm from the top of the LN. When setting up an artery for imaging, focus to the top of the adventitia (autofluorescent connective tissue) and then z-step down through the tissue to image at a known depth (Fig. 2 C-F).
Lamina adventitia is a major site of arterial wall lymphocyte infiltration into atherosclerotic arteries; typically this is around 0--30 μm from the top of the vessel. Lymphocyte infiltration is randomly distributed throughout the arteries.
15. Typically scan an area of 256 by 256 pixels (284 μm by 284 μm) in x and y , with z -depth of 35--50 μm (in 2.55 μm steps)
16. The depth of the stack imaged is determined by how fast cells are moving in the LN--faster cells require fast imaging in order to track in software.

Generally, imaging a cell once every ~30 seconds is sufficient for accurate tracking.

Acknowledgments

The authors would like to thank Dr. Gary Dever (Centre for Biophotonics, Strathclyde Institute of Pharmacy & Biomedical Sciences, University of Strathclyde) for the experimental support. This work was supported by a BHF project grant (PG/06/083/21198 awarded to PG, JMB, PM and Prof Iain McInnes) and from Wellcome trust project grants (GR066890MA awarded to JMB, PG and Prof R.S. Phillips; GR068895 awarded to PG, JB, Prof. A. Gurney, Mr. D. Wokosin). PM is supported by a Capacity Building Award in Integrative Mammalian Biology funded by the BBSRC, BPS, KTN, MRC and SFC. OM is funded through an RCUK fellowship.

5. References

- 1- Robertson, A. K., Hansson, G. K. (2006) T cells in atherogenesis: for better or for worse? *Arterioscler Thromb Vasc Biol.* **26**, 2421-32.
2. Hansson, G. K., Libby, P. (2006) The immune response in atherosclerosis: a double-edged sword. *Nat Rev Immunol.* **6**, 508-19.
3. Hugues, S., Fetler, L., Bonifaz, L., Helft, J., Amblard, F., Amigorena, S. (2004) Distinct T cell dynamics in lymph nodes during the induction of tolerance and immunity. *Nat Immunol.* **5**, 1235-42.
4. Shakhar, G., Lindquist, R. L., Skokos, D., Dudziak, D., Huang, J. H., Nussenzweig, M. C., Dustin, M. L. (2005) Stable T cell-dendritic cell interactions precede the development of both tolerance and immunity *in vivo*. *Nat Immunol.* **6**, 707-14.
5. Zinselmeyer, B. H., Dempster, J., Gurney, A. M., Wokosin, D., Miller, M., Ho, H., Millington, O. R., Smith, K. M., Rush, C. M., Parker, I., Cahalan, M., Brewer, J. M., Garside, P. (2005) *In situ* characterization of CD4⁺ T cell behaviour in mucosal and systemic lymphoid tissues during the induction of oral priming and tolerance. *J Exp Med.* **201**, 1815-1823.
6. Millington, O. R., Gibson, V. B., Rush, C. M., Zinselmeyer, B. H., Phillips, R. S., Garside, P., Brewer, J. M. (2007) Malaria impairs T cell clustering and immune priming despite normal signal 1 from dendritic cells. *PLoS Pathog.* **3**, 1380-7.
7. Miller, M. J., Wei, S. H., Parker, I., Cahalan, M.D. (2002) Two-photon imaging of lymphocyte motility and antigen response in intact lymph node. *Science* **296**, 1869-73.
8. Mempel, T. R., Henrickson, S. E., Von Andrian, U.H. (2004) T-cell priming by dendritic cells in lymph nodes occurs in three distinct phases. *Nature* **427**, 154-9.

9. Miller, M. J., Hejazi, A. S., Wei, S. H., Cahalan, M. D., Parker, I. (2004) T cell repertoire scanning is promoted by dynamic dendritic cell behavior and random T cell motility in the lymph node. *Proc Natl Acad Sci USA* **101**, 998-1003.
10. Celli, S., Garcia, Z., Bousso, P. (2005) CD4 T cells integrate signals delivered during successive DC encounters *in vivo*. *J Exp Med.* **202**, 1271-8.
11. Schneider, H., Downey, J., Smith, A., Zinselmeyer, B. H., Rush, C., Brewer, J. M., Wei, B., Hogg, N., Garside, P., Rudd, C. E. (2006) Reversal of the TCR stop signal by CTLA-4. *Science* **313**, 1972-5.
12. Millington, O. R., Zinselmeyer, B. H., Brewer, J. M., Garside, P., Rush, C. M. (2007) Lymphocyte tracking and interactions in secondary lymphoid organs. *Inflamm Res.* **56**, 391-401.
13. Okada, T., Miller, M. J., Parker, I., Krummel, M. F., Neighbors, M., Hartley, S. B., O'Garra A., Cahalan M. D., Cyster J. G. (2005) Antigen-Engaged B Cells Undergo Chemotaxis toward the T Zone and Form Motile Conjugates with Helper T Cells. *PLoS Biol.* **3**, e150.
14. Garside, P. and Brewer, J. M. (2008) Real-time imaging of the cellular interactions underlying tolerance, priming, and responses to infection. *Immunol Rev.* **221**, 130-46.
15. Matheu, M. P., Parker, I., Cahalan, M. D. (2007) Dissection and 2-Photon Imaging of Peripheral Lymph Nodes in Mice. *Journal of Visualized Experiments* <http://www.jove.com/index/Details.stp?ID=265>
16. Maffia, P., Zinselmeyer, B. H., Ialenti, A., Kennedy, S., Baker, A. H., McInnes, I. B., Brewer, J. M., Garside, P. (2007) Images in cardiovascular medicine. Multiphoton microscopy for 3-dimensional imaging of lymphocyte recruitment into apolipoprotein-E-deficient mouse carotid artery. *Circulation* **115**, e326-8.

17. Celli, S., Lemaitre, F., Bousso, P. (2007) Real-time Manipulation of T Cell-Dendritic Cell Interactions *In vivo* Reveals the Importance of Prolonged Contacts for CD4⁺ T cell Activations. *Immunity* **27**, 625-634.
18. Galkina, E., Kadl, A., Sanders, J., Varughese, D., Sarembock, I. J., Ley, K. (2006) Lymphocyte recruitment into the aortic wall before and during development of atherosclerosis is partially L-selectin dependent. *J Exp Med.* **203**, 1273-82.
19. Matheu, M. P., Cahalan, M. D. (2007) Isolation of CD4⁺ T cells from Mouse Lymph Nodes using Miltenyi MACS Purification. *Journal of Visualized Experiments* <http://www.jove.com/index/Details.stp?ID=409>
20. Huang, J. H., Cárdenas-Navia, L. I., Caldwell, C. C., Plumb, T. J., Radu, C. G., Rocha, P. N., Wilder, T., Bromberg, J. S., Cronstein, B. N., Sitkovsky, M., Dewhirst, M. W., Dustin, M. L. (2007) Requirements for T lymphocyte migration in explanted lymph nodes. *J Immunol.* **178**, 7747-55.

Figure Legends

Figure 1

Procedure for ex vivo imaging of LN. Isolated LNs are adhered to unbreakable plastic coverslips (A) using veterinary-grade superglue (B). The LN is rolled on blue roll to remove fat (C). A thin layer of Vetbond is spread over slide using tissue paper (D & E) and the LN secured on this (F). The glue is cured by immersing in media (G) before trimming the slide to size (H). Finally, a small amount of grease is spread on the underside of the coverslip to secure in the imaging chamber (I).

Figure 2

Dissection of the brachiocephalic artery (A) and vessel isolation for imaging (B). Several red labelled lymphocytes are detectable mainly in adventitia (C, D, E, ~10-30 μm below the outer surface) and within the autofluorescent elastic fibres (green) in the tunica media (F, ~30-50 μm below the outer surface) as shown by the set of longitudinal sections of ApoE^{-/-} mouse brachiocephalic artery.

Figure 3

Analysis of T cell migration and interactions in the LN. Using software, individual cells are identified within the 3D image and then tracked over time (A). Multiple cell tracks can be plotted relative to each other to effectively show migration distances or polarized movement (B). The velocity of each track can then be graphed to compare the movement of different samples (e.g. to show the difference between naïve T cells and those recognizing antigen (C). Alternatively, the amount of interaction between red T cells and green DCs can be calculated as a colocalization coefficient and compared between two different samples (D).

Figure 1: Millington, Brewer, Garside & Maffia

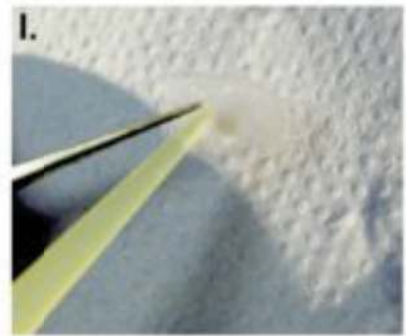
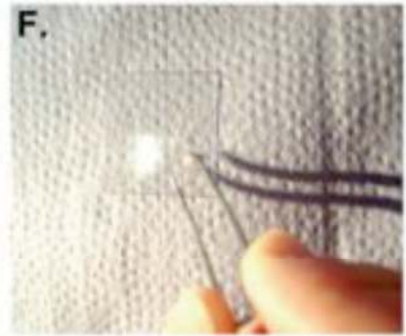
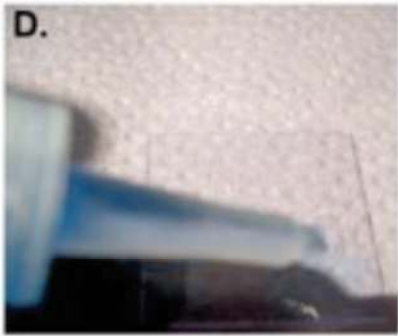


Figure 2: Millington, Brewer, Garside & Maffia

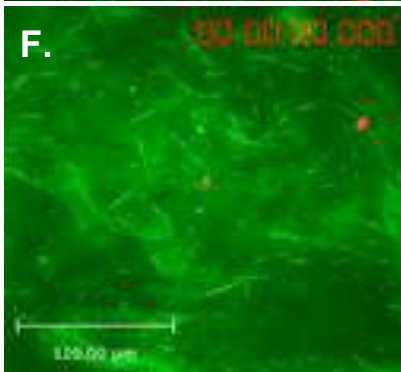
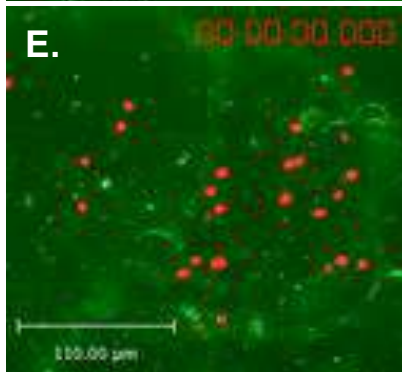
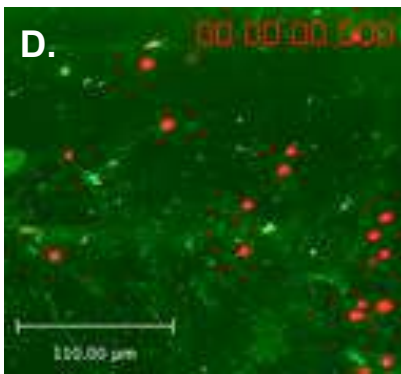
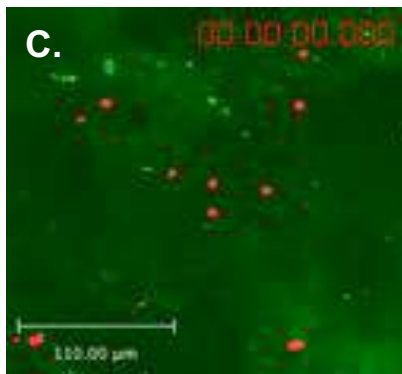
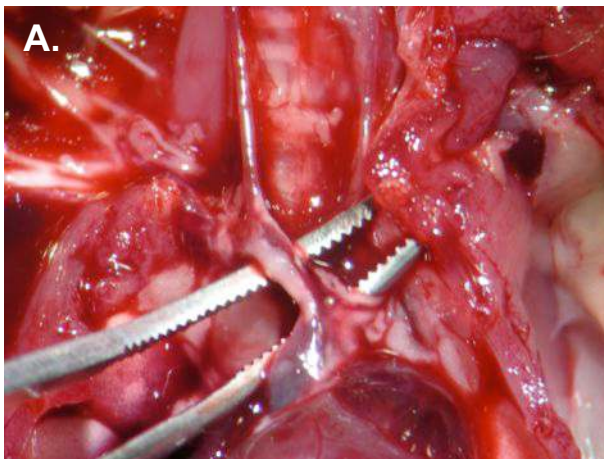


Figure 3: Millington, Brewer, Garside & Maffia

